Springer

KSME

Journal of Mechanical Science and Technology 24 (10) (2010) 2007~2016
www.springerlink.com/content/1738-494x
DOI 10.1007/s12206-010-0705-9

The cavitation behavior with short length blades in centrifugal pump †

Quangnha Thai and Changjin Lee*

Department of Aerospace Information Engineering, Konkuk University, 1 Hwayang-dong, Gwangjin-gu, Seoul 143-701, Korea

(Manuscript Received September 3, 2009; Revised May 31, 2010; Accepted June 23, 2010)

Abstract

A CFD code with 2-D cascade model was developed to predict the cavitation behavior around the impeller blades of impeller in a centrifugal pump. The governing equations are the two-phase Reynolds Averaged Navier-Stokes equations in a homogeneous form in which both liquid and vapor phases are treated as incompressible fluid. To close the model, a standard k-ε turbulence model is introduced. And the mass transfer rates between liquid and vapor phases are implemented as well. The validations are carried out by comparing with reference data in impeller of a centrifugal pump impeller. The cavitation characteristics of current centrifugal pumps is tested at an on-design point (V=8 m/s) and two off-design points (V=20 m/s and V=30 m/s), respectively. The criteria of cavitation and flow instability around blades are presented. The results show that the current centrifugal pump can safely operate without cavitation at on-design point. Also, the simulation shows cavitation develops inhomogeneously among the blades at off-design points. Moreover, the effects of additional blades in the impeller are studied as well. From the numerical results, it is expected that a half-length blade is the optimum configuration as additional blades in cavitation point of view.

Keywords: Cavitation; Half-length blade; 2-D cascade; Centrifugal pump; Impeller

1. Introduction

Cavitation is a phenomenon in which liquid evaporates and vapor bubbles occur in the region where the pressure of the liquid falls off under vapor pressure. It is usually observed in high-speed fluid machinery such as propellers, pumps, and impeller blades where the flow accelerates and the pressure decreases. Cavitation can give rise to erosion damage, noise, vibration and hydraulic performance deterioration by periodic inception, growth, depletion of vapor bubbles. Specially, cavitation in a centrifugal pump reduces efficiency and causes pressure head damage. The understanding of cavitating flow is one of the common subjects for designers of high-speed fluid machinery. The flow in a centrifugal pump is intrinsically turbulent, 3-D and unsteady; sometimes cavitation appears. The design of centrifugal pump is mainly based on the steady-state theory, empirical correlation, combination of model testing, and engineering experiences. Over the last few years, however, with the development of the computer, there have been many researches on the centrifugal pump in numerical calculation. Croba et al. [1] considered a more realistic through 2-D, unsteady, incompressible and turbulent flow. Anagnostopoulos (2006) [2] simulated the 3-D turbulent flow in a centrifugal pump impeller with Cartesian grid to represent an adequate accuracy for the complex geometry of the centrifugal pump impeller. Cheah et al. (2007) [3] simulated the complex internal flow in a centrifugal pump impeller with six twisted blades by using 3-D Navier-Stokes code with a standard k-ε two-equation turbulence model. Different flow rates were specified at the inlet boundary to predict the characteristics of the pump such as impeller passage flow, flow separation and pressure distribution.

As aforementioned, cavitation in an impeller is naturally a 3-D phenomenon. However, due to the quite intrinsic complex nature with phase change, a mathematical model and numerical method are considerably difficult to establish. Generally, the pump is designed to operate with non-zero incidence angle at a nominal flow rate. Nevertheless, in the range of operational conditions, the angle of attack of impeller blades remains very small, because of variable flow thread and the associated curvature of blades. The back flow at the inlet may happen sometimes but it's not strong. So, the approach of a 2-D cascade can be adopted. The cavitation in a 2-D cascade calculation has been investigated by many researchers so far, instead of 3-D calculation. For example, Joussellin et al. [4] simulated rotating cavitation and alternate blade cavitation occurring four-blade cyclic cascade by applying 2-D unsteady numerical method incorporated with cavitation model by barotropic state law. Iga et al. [5] simulated propagating phenomena of cavitation, which corresponds to the rotating cavi-

† This paper was recommended for publication in revised form by Associate Editor Won-Gu Joo

* Corresponding author. Tel.: +82 2 450 3533, Fax: +82 2 444 6106
E-mail address: cjlee@konkuk.ac.kr

tation through three-blade cyclic cascade and discussed the difference of the results obtained in different conditions at the inlet boundary. And the collaborative work of French researchers [6, 7] carried out the numerical and experimental analysis about cavitation behavior of four-blade inducer using a 2-D model of unsteady cavitating flow in a blade cascade.

For the reduction of computing time and analysis in design, the 2-D cascade looks like a new technique to 3-D calculation of cavitation analysis. Based on the prediction of 2-D cascade, a clearer understanding can be expected for 3-D cavitation. This is the reason why the present paper would like to simulate cavitation around pump blades by using the 2-D cascade. We are interested in simulating the cavitation behavior around blades of impeller in centrifugal pump. The main objective is to establish the criterion of cavitation inception, the influence of the interaction among cavitations in flow passages. And, the effect of additional blades in impeller of centrifugal pump is also investigated by evaluating the characteristics of cavitation including the area of cavitation region and the fluctuation of mass flow rate. The benefits and disadvantages when putting the additional blades will be discussed in this study as well.

2. Governing equations and numerical procedure

2.1 Governing equations

The vapor-liquid flow is described by a single-fluid model which is treated as a homogeneous bubble-liquid mixture. The set of governing equations under single-fluid model comprises the conservative form of Reynolds-averaged Navier-Stokes equations, the k-ε two-equation turbulence closure and a transport equation for the liquid volume fraction. The continuity, momentum and liquid volume fraction equations are written in Cartesian coordinate system as follows:

$$\frac{\partial}{\partial t}\int_V \rho_m dV + \int_S \rho_m \vec{v}.\vec{n}dS = 0 \tag{1}$$

$$\frac{\partial}{\partial t}\int_V \rho_m \vec{v}dV + \int_S \rho_m \vec{v}\vec{v}.\vec{n}dS = \int_S \vec{T}.\vec{n}dS + \int_V \rho_m \vec{b}dV \tag{2}$$

$$\frac{\partial}{\partial t}\int_V \alpha_l dV + \int_S \alpha_l \vec{v}.\vec{n}dS = \int_V \left(\dot{m}^+ + \dot{m}^-\right)dV \tag{3}$$

where

$$T_{ij} = -\left(p + \frac{2}{3}(\mu+\mu_t)\frac{\partial u_j}{\partial x_j}\right)\delta_{ij} + (\mu+\mu_t)\left(\frac{\partial u_i}{\partial x_j} + \frac{\partial u_j}{\partial x_i}\right)$$

The constitutive relations for the density and dynamic viscosity of the mixture are:

$$\rho_m = \rho_l\alpha_l + \rho_v(1-\alpha_l) \quad \text{and} \quad \mu = \mu_m = \mu_l\alpha_l + \mu_v(1-\alpha_l)$$

And the turbulent viscosity is defined as follows:

$$\mu_t = \frac{\rho_m C_\mu k^2}{\varepsilon}$$

2.2 Cavitation model

Cavitation terms, based on Kunz et al.'s model [8], are used in this study. The evaporation and condensation rates are given as follows:

$$\dot{m}^- = \frac{C_{dest}\rho_v\alpha_l MIN[0, p-p_v]}{\rho_l\left(\frac{1}{2}\rho_l U_\infty^2\right)t_\infty}$$

$$\dot{m}^+ = \frac{C_{prod}\rho_v\alpha_l^2(1-\alpha_l)}{\rho_l t_\infty}$$

where $C_{prod} = 9\text{x}10^5$, $C_{dest} = 3\text{x}10^4$, $t_\infty = 1$

2.3 Numerical procedure

The discretization of the governing Eqs. (1), (2), (3) is done by using finite volume method. And the collocated grid system is used to allocate velocity components and dependent variables. The convective and diffusive terms are differenced by upwind scheme and central scheme, respectively. The solution of pressure and velocity may show an unphysical oscillation due to the use of collocated grid system and should be treated by using interpolation in the momentum equation to avoid oscillation. Details of the numerical description can be found in the reference [9].

2.4 2-D cascade and boundary condition

Analyzing the flow field data will provide deep insights into the flow mechanism. 2-D cascade flow was adopted as the methodology for flow analysis in this study. The 2-D blade-to-blade cascade was drawn by cutting the 3-D inducer geometry at constant radius equal to 70% of the tip radius as shown in Fig. 1. Details are found in the reference [10]. The axial flow entrance combines the rotational speed of the blades and will result in the relative velocity between flow and blades. In the present 2-D calculation, the blades are considered stationary and the relative flow comes to blades with a certain angle of attack. The boundary conditions used in the present simulations includes inflow, outflow, non-slip, and periodic boundary condition. At the inlet, the velocity and liquid fraction are imposed and the pressure is extrapolated from the interior points. At the downstream, pressure is imposed while the other variables are extrapolated. At the wall, the velocity is zero while the other variables are extrapolated from the interior points. Along the lines which separate the blades, all variables are extrapolated from the interior points. The periodic condition is applied between the 4th and 1st passages. Dummy cell must be imagined as similar as possible to the cells of the original corresponding row to consider a periodic boundary

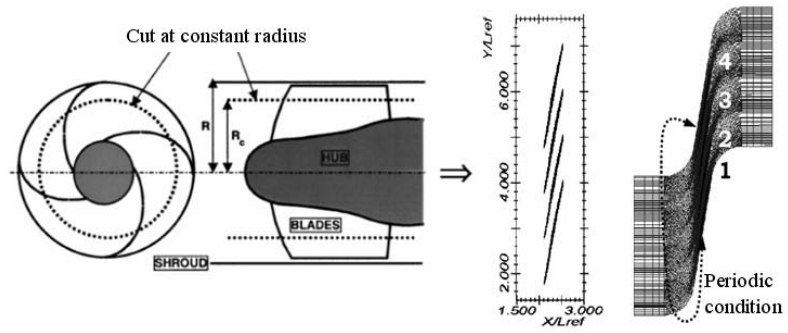

Fig. 1. 2-D cascade modeling [10].

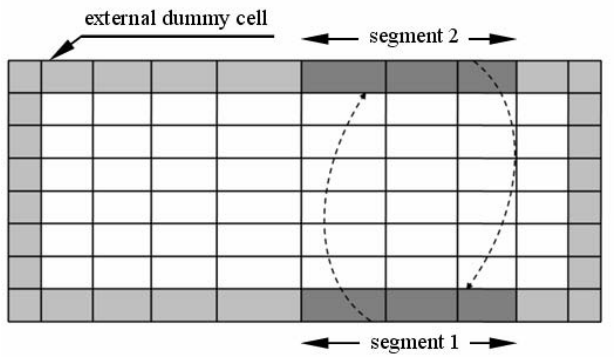

Fig. 2. Variables transfer between segment 1 and segment 2 in periodic boundary condition.

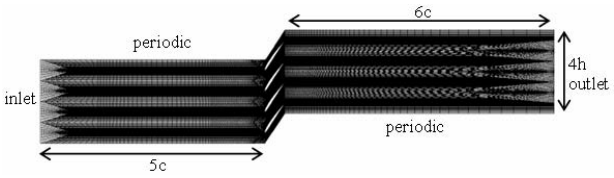

Fig. 3. Cascade domain and boundary condition.

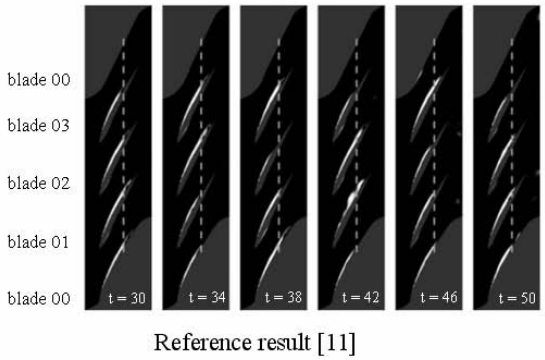

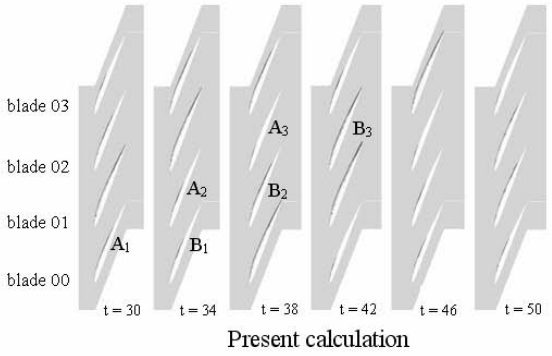

Fig. 4. Comparison of instantaneous flow field through contour of liquid volume fraction.

condition. The variables must be transferred according to the arrows shown in the Fig. 2. Two lines on the segment 1 must be transferred to two corresponding lines on segment 2.

3. Code verification

3.1 Cavitating flow in a pump inducer with 2-D cascade model

A 2-D four-blade cascade is considered to check the validity of our in-house code. The computational domain, boundary condition in the calculation is described in Fig. 3. The blade cross section is Clark Y-6%; pitch chord ratio and stagger angle of hydrofoil are 1.62 and 64.27^0, respectively. The working fluid is pure liquid water ($\alpha_l = 1$) which comes to the blade cross section with the velocity of 34.54 m/s and angle of attack of 4^0. Reynolds number is fixed as $5x10^5$ [11]. The pump inducer is operated under standard pressure and the cavitation number is 0.5.

Fig. 4 shows instantaneous flow field with cavity indicated by volumetric fraction and all flow passage filled with liquid is modified in gray color instead of red color in the present calculation to highlight the cavitation region. Since the blade rotation was captured by 2-D cascade modeling, the sequence of cavitation behavior can be examined by the variation of size on consecutive blades from the first. The cavitation on blade A_1 collapses on blade A_2 and then continues collapsing on

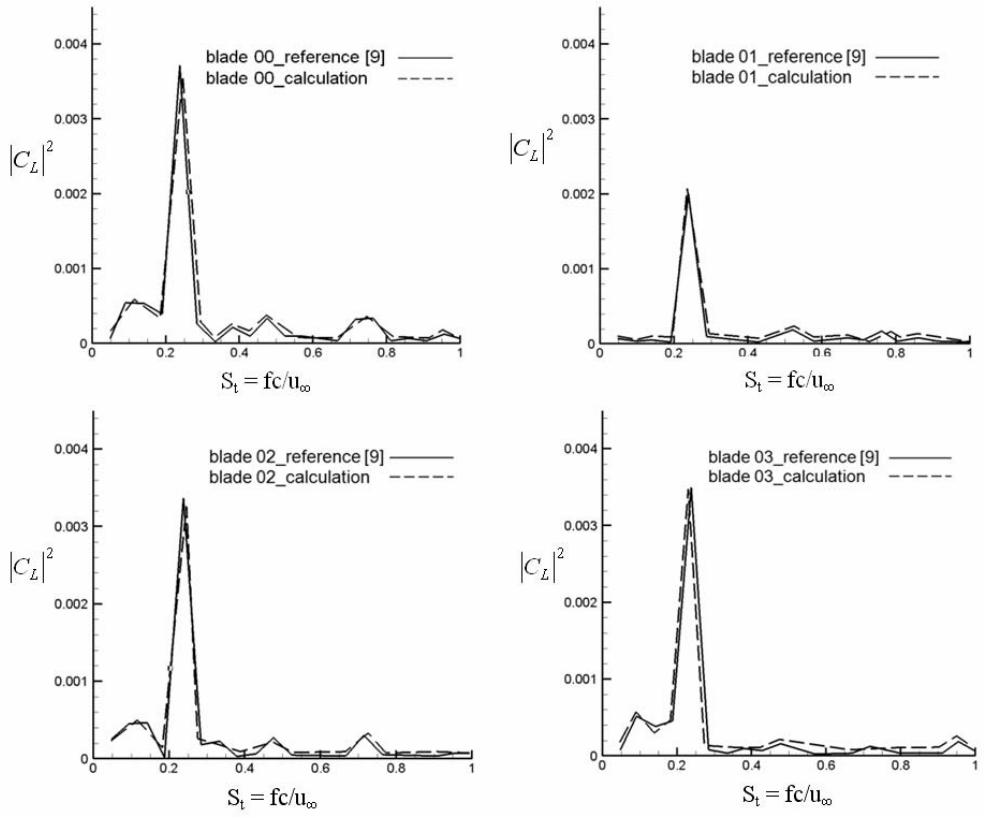

Fig. 5. Comparison of spectrum of Strouhal number of lift coefficient fluctuation.

blade A_3 or the cavitation on blade B_1 develops on blade B_2, and then continues developing on blade B_3. The growth and depletion of cavitation causes flow instability in the flow. The good agreement of spectrum of Strouhal number of lift coefficient fluctuation can be found by the comparison with reference result [11] as shown in Fig. 5. The intensity of fluctuation is very large at $S_t = 0.25$ and then becomes smaller as the increase in frequency. This means that the sheet cavitations among the passages are inhomogeneous at the beginning of the calculation, but gradually become more homogeneous due to the gradual decrease of the fluctuation. If the flow condition reaches to steady, the intensity of the fluctuation will diminish to a lower limitation. In other words, the smallest fluctuation is obtained in steady. In this case, the fluctuation still remains but the intensity is smallest.

3.2 Unsteady flow in impeller using 2-D cascade model

Recently, Kitano Majidi solved the unsteady 3-D viscous flow in entire impeller and volute casing of a centrifugal pump and showed the result of mass flow rate fluctuation through the blade passages [12]. The present paper would like, for verification purpose, to make sure that the in-house code can catch the characteristics of cavitation not only on the hydrofoil in a pump inducer but also on the blades in a centrifugal pump. The original model of a commercial impeller in reference [12] is shown in Fig. 6. It is shrouded and has five backswept

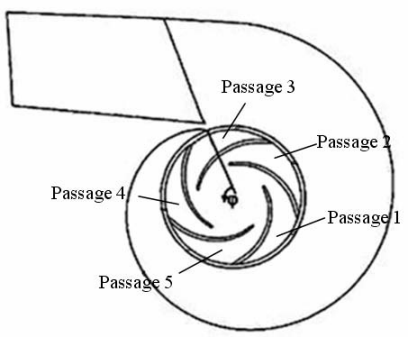

Fig. 6. Blade passage and casing [12].

blades. The blade profile varies between the hub and the shroud. The blade angle at the inlet varies from 18.5^0 at the shroud to 30^0 at the hub; the blade angle at the outlet is 23.5^0. The outlet diameters, outlet passage width of impeller are 508 mm, 72.5 mm, respectively. And the base circle diameters, volute width at the base circle of volute casing are 523 mm, 94.3mm, respectively. At the design point, the mass flow rate, total head, rotational speed and specific speed are 730.0 kg/s, 46.68 m, 1482 rpm, 68 min^{-1} respectively. Details are found in Table 1 of reference [12].

A 1780x30 structured mesh is generated; the boundary condition and the numerical method of the calculation are similar to the previous one. The water flow comes to the inlet of the passages with a velocity of 6 m/s. The centrifugal pump is

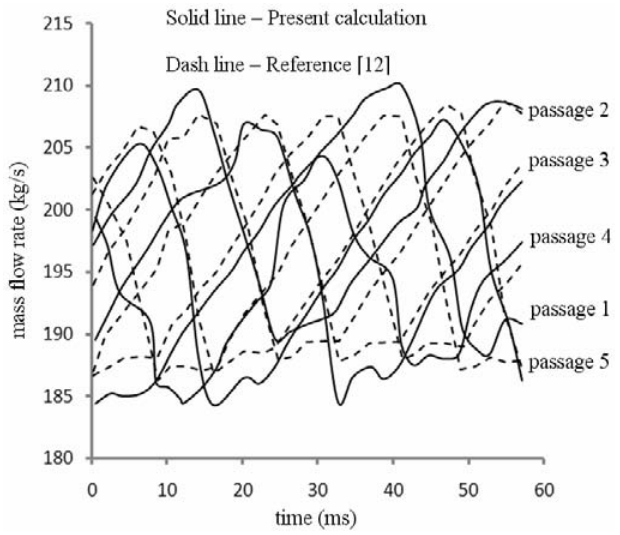

Fig. 7. Unsteady mass flow rate through each passage.

operated in standard pressure condition. The mass flow rate at right after blades in term of time is investigated to compare the present result with reference. As seen in Fig. 7, the same tendency of unsteady flow rate in each passage can be observed although the result of the present calculation is not so close to the reference. The main reason for the difference between two results here is due to different methods adopted in each calculation (3-D calculation in reference paper versus 2-D cascade calculation in the present paper). However, it can be seen that the 2-D cascade model can catch a fairly good prediction of cavitation compared to the 3-D approach.

4. Results and discussion

4.1 Cavitation around the blades of impeller using 2-D cascade

The centrifugal pump in this study is for feeding fuel JP-7; the configuration of impeller is shown as Fig. 8. The blades have two circular arcs shape, 0.5mm thickness (s) and 18mm chord length (c). The outer (d_2) and inner diameters (d_1) are 60 mm and 21 mm, respectively. And the inlet (β_{s1}) and outlet (β_{s2}) angle of blades are 15^0 and 23^0. There are 3 blades and 3 half-length blades with the passage width (h) of 11.25 mm. The rotational speed (n) is 5660rpm. This centrifugal pump usually operates at the on-design point at which the inlet velocity and standard temperature are 8 m/s and 20^0C, respectively. The operational temperature range of this centrifugal pump varies from -35^0C to 43^0C and corresponding value of density, dynamics viscosity and velocity tabulated as shown in Table 1.

The pump impellers considered in the present paper are shown as Fig. 9. The cavitation behavior around blades of pump impeller without half-length blades is investigated at first and then, the pump impeller with half-length blades is also considered to study the role of half-length blades. The method and techniques applied in this calculation are described in the previous section 2.4. Steady cavitation is investigated and the result can be observed in Fig. 10. At the on-design point, the result shows there is no cavitation. However, symmetrical and stable cavitation occurs at the suction side of each blade at the off design point. From the on-design point, increasing the velocity until around 20 m/s, the inception of

Table 1. Operational range of centrifugal pump.

Temperature (^{0}C)	Density (kg/m^3)	Dynamic viscosity (kg/m.s)	Velocity (m/s)
-35	838.15	0.006727	6
20	795.948	0.0009375	8
43	781.218	0.0011925	10

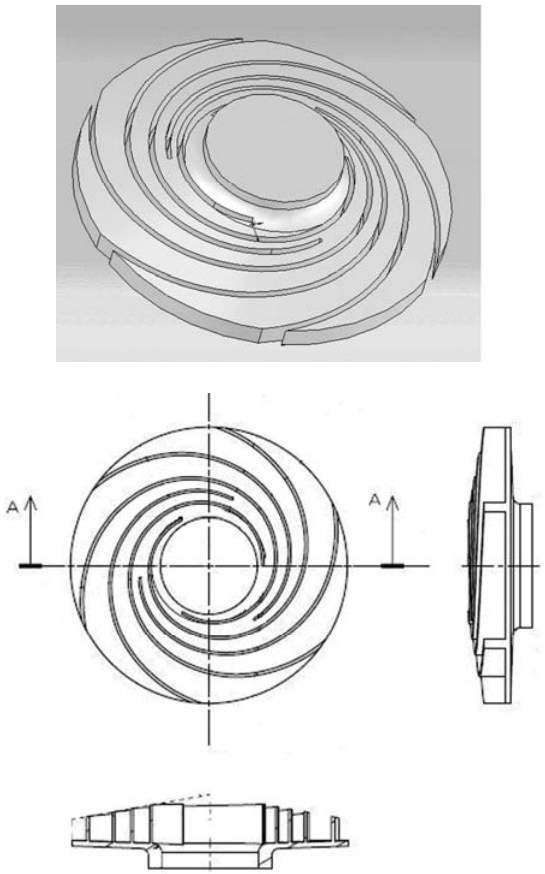

Fig. 8. 3-D geometry and projections of impeller.

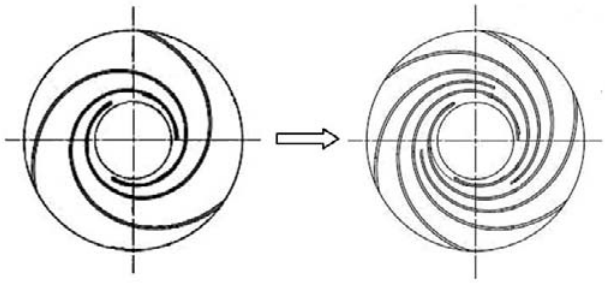

Fig. 9. Configuration of pump impeller without and with half-length blades.

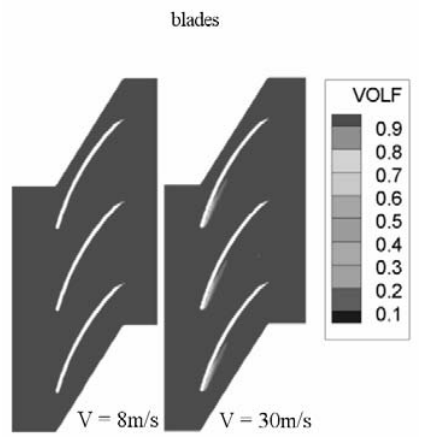

Fig. 10. Cavitation shape of steady calculation at on and off design point.

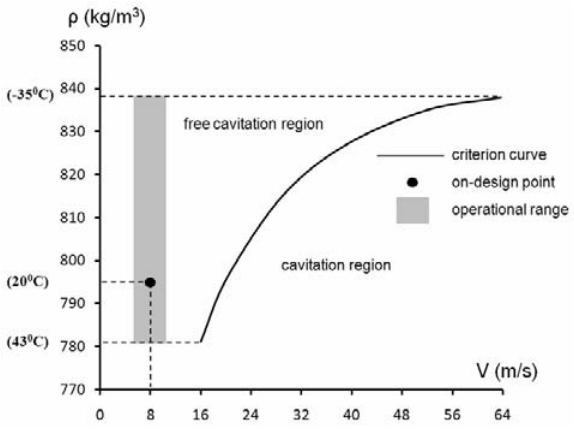

Fig. 11. Criterion curve of cavitation inception.

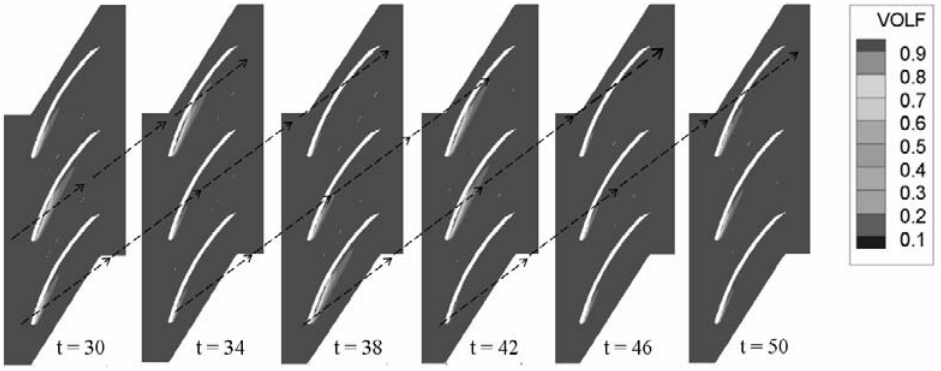

Fig. 12. Instantaneous flow field represented by contour of liquid volume fraction at off-design point.

cavitation was found. And steady calculation is carried out again by gradually increasing velocity. Finally, we obtained the criterion curve of cavitation as shown in Fig. 11. The big black point and the rectangular box depict the condition at the on-design point and the operational range of this centrifugal pump, respectively. It's obvious that this centrifugal pump operates in a safe region without appearance of cavitation.

Sometimes the operating conditions of a centrifugal pump may not be at the on-design point due to rotating speed or temperature variation. So, the unsteady cavitating flow at certain off design point is studied as well and an arbitrary velocity of 30 m/s is picked up in the calculation. The instantaneous flow field represented by the contour of liquid volume fraction is investigated and the result is obtained as Fig. 12. The sheet cavitation among blades at the suction side is not symmetrical anymore as in the steady calculation. It develops inhomogeneously due to flow rate variation through the passages. The growth and depletion of cavitation are created and move from one blade to next blade according to the arrow in Fig. 12. And it causes the instability of the blade cascade.

4.2 The role of half-length blades

Another interesting issue has been studied to define the role of the half-length blades in a centrifugal pump impeller. As aforementioned, the cavitation occurred at off-design points at which velocity is large enough. The present paper is interested in defining the cavitation inception in terms of velocity and length of additional blades. So, the area of cavitation region is investigated in the calculation. And Fig. 13 on the top shows the reduction of cavitation region due to the imposition of additional blades. With half-length blades, we can expect the minimum cavitation area compared to the other cases. The bottom graphs gives a clear visualization of cavitation shape in the case with half-length blades, and the black region was zoomed in to have a better observation as shown in the two bottom figures. It is obviously seen that cavitation size at the velocity of 20 m/s is smaller than that at 30 m/s corresponding to the smaller value in the Fig. 13 on the top.

In reality, when cavitation occurs, there is back flow on the pressure side of the full blades. The occurrence of cavitation is the main reason creating the backflow. The larger the cavitation region is, the stronger back flow is going to be. When some appropriate additional blades are located between full blades, the back flow from the pressure side of full blades will touch the suction side of the additional blades. It seems to be that the back flow has something to catch and moves along the curve of additional blades suction side instead of moving back

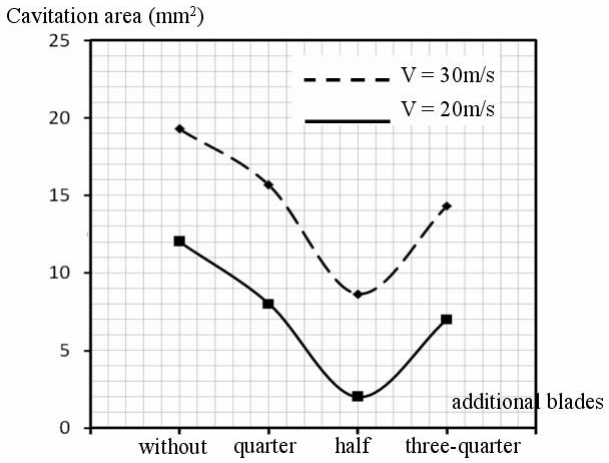

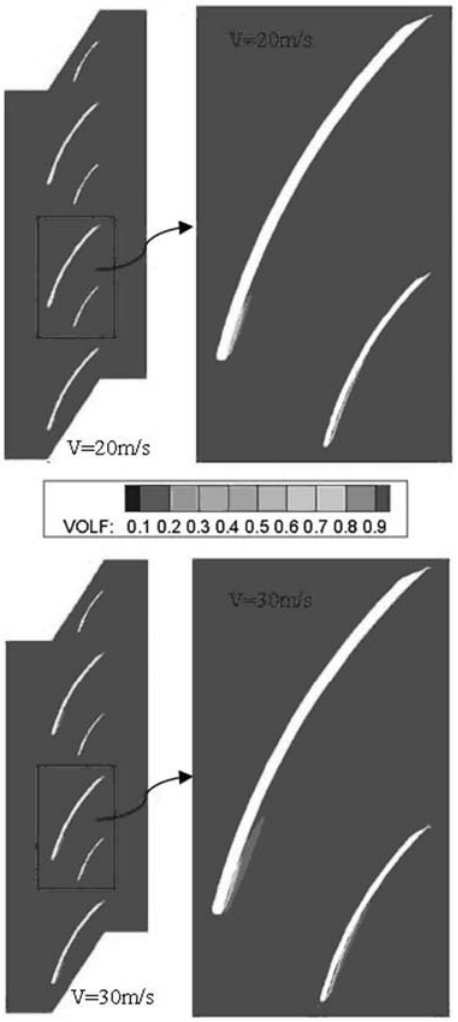

Fig. 13. Comparison of area of cavitation region and visualization of cavitation at two off-design points.

to the leading edge of full blades. That's the reason why the back flow near the middle of full blade pressure side can't be moved back to the leading of the blade and is pushed downstream to the additional blade suction side. Then, the back

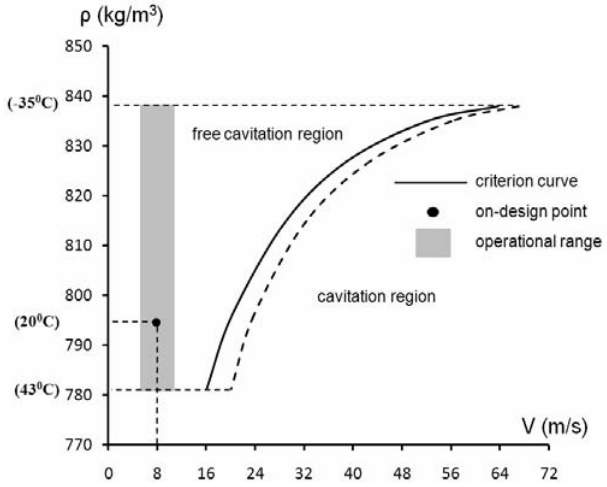

Fig. 14. Comparison of cavitation criterion curve.

flow between pressure side of full blade and suction side of additional blade is going to be weaker. Moreover, the flow has a tendency to move toward the trailing edge of the additional blade by passing through its pressure side. These additional blades indirectly reduce cavitation by reducing backflow or flow instability. The result shows that the optimum length of the additional blade should be a half of a full blade. Another benefit of the half-length blades is found as shown in Fig. 14. The non-cavitation region is improved and a little bit wider than that in the case without half-length blades. This centrifugal pump more safely operates. For example, in the case without the addition of three half-length blades into impeller and at standard operational temperature condition (20℃), the inception of cavitation happens if velocity is increased up to 20 m/s. However, it doesn't appear yet if three half-length blades are added into this pump impeller. The pump still operates freely from cavitation. In this operational condition, the pump is still safe from cavitation. This is one of the benefits of adding three half-length blades into impeller. The velocity which makes centrifugal pump susceptible to cavitation can be delayed up to 23 m/s, instead of 20 m/s in case without half-length blades.

The fluctuation of mass flow rate downstream of the blades is also important in the safe operation of a centrifugal pump. That's why FFT analysis of the fluctuation of mass flow rate is investigated as well in this paper. In Fig. 15, results at the on-design point are shown with various lengths of additional blades. Generally with additional blades, the fluctuations are weaker than that without additional blades. However, it is a little higher at some certain frequency. At low and high frequency, the comparison can be easily observed in Fig. 16 and Fig. 17, respectively. With half-length blades, the amplitude of the fluctuation around 2000 Hz is much smaller compared to the other cases. For a centrifugal pump, large fluctuations at high frequency affect destructively to the safe operation and structure. So, the addition of half-length blades contributes the flow to be stable by eliminating high frequency oscillations of mass flow rate.

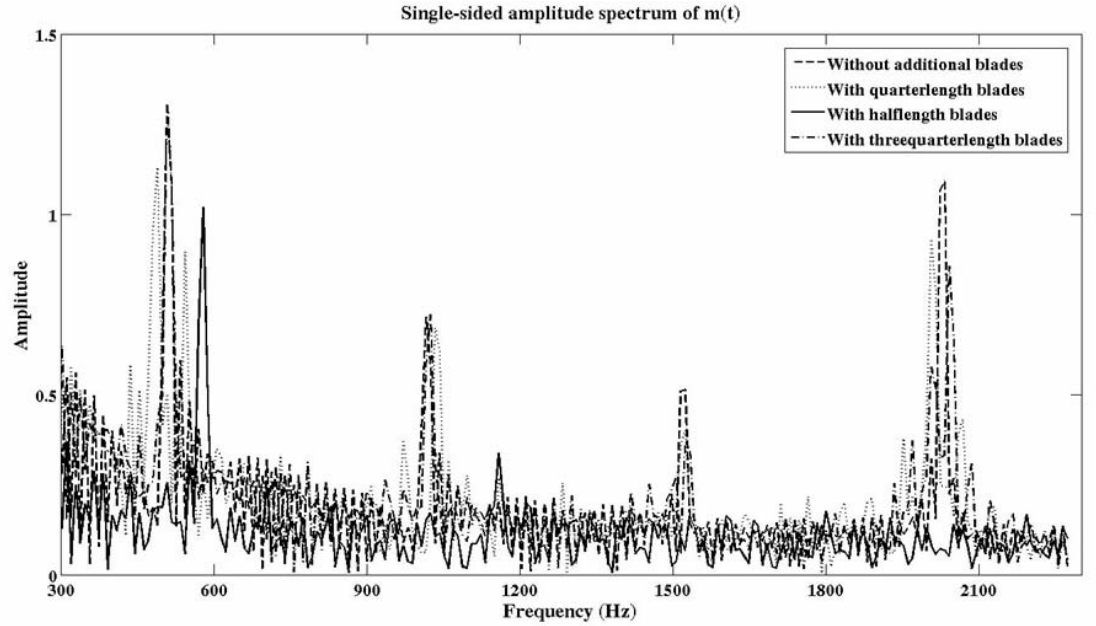

Fig. 15. Comparison of mass flow rate fluctuation at on-design point.

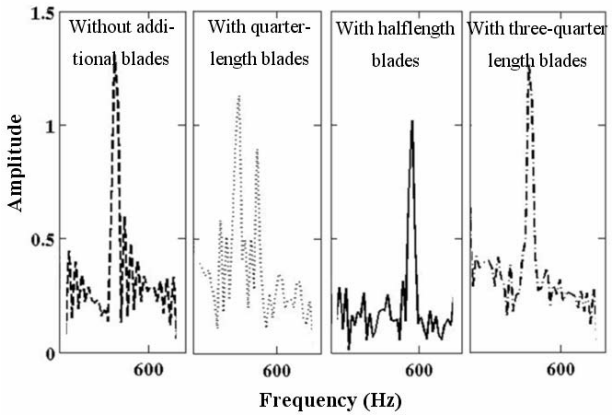

Fig. 16. Comparison of mass flow rate fluctuation at low frequency at on-design point.

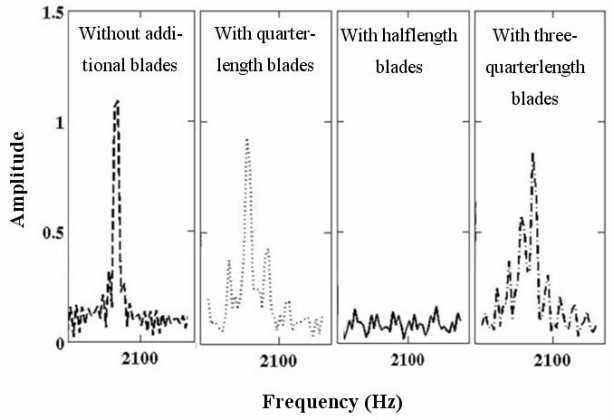

Fig. 17. Comparison of mass flow rate fluctuation at high frequency at on-design point.

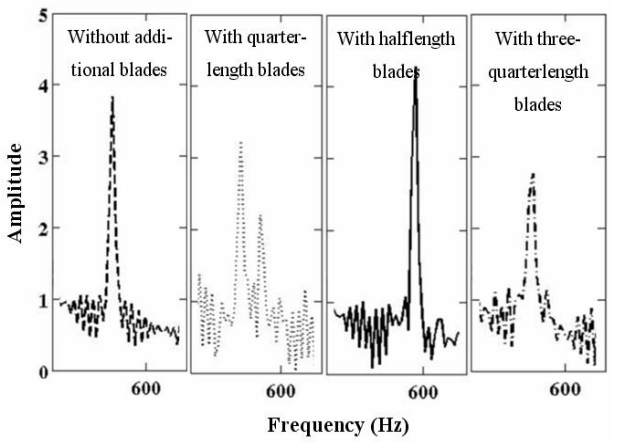

Fig. 18. Comparison of mass flow rate fluctuation at low frequency at off-design point V = 20 m/s.

Fig. 19 and Fig. 21 also show nearly the same tendency of characteristics of amplitude at high frequency as observed with half-length blades at two different off-design points. However, higher fluctuation is observed at low frequency around 500 Hz in Fig. 18 and Fig. 20. This centrifugal pump is still fine even though it operates under unsteady conditions. By adding three half-length blades into the impeller, the centrifugal pump can be expected to have more stable operational characteristics for the entire operational range. Within the operational range, additional blades contribute the flow to be more stable by suppressing the high frequency fluctuations. Even for out of range, additional blades reduce cavitation size, high frequency oscillation and improve non-cavitation region.

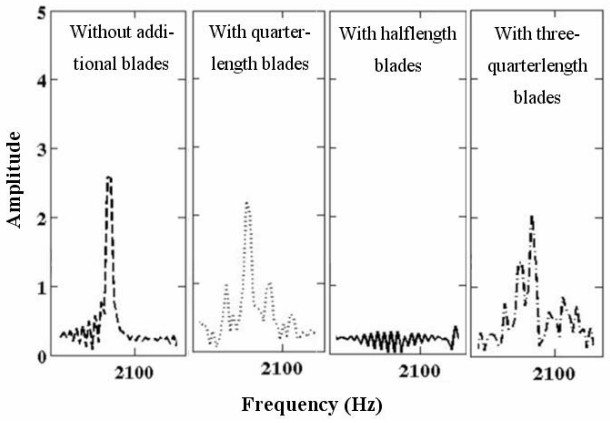

Fig. 19. Comparison of mass flow rate fluctuation of high frequency at V = 20 m/s.

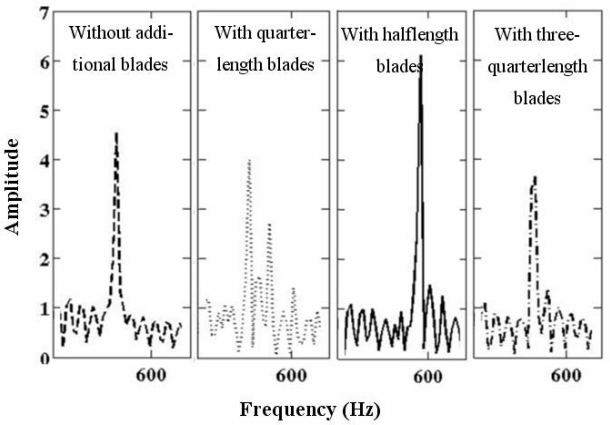

Fig. 20. Comparison of mass flow rate fluctuation of low frequency at V = 30 m/s.

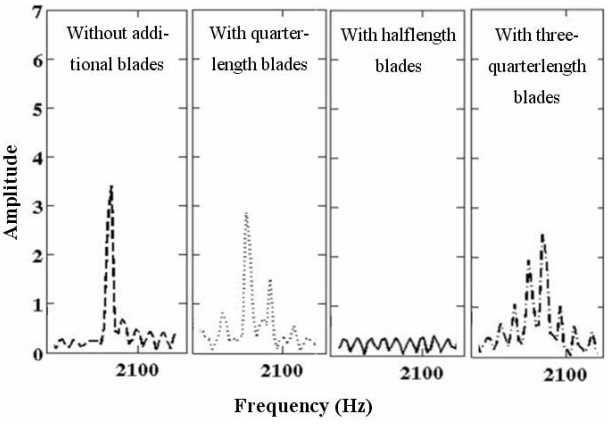

Fig. 21. Comparison of mass flow rate fluctuation of high frequency at V =30 m/s.

5. Summary and conclusion

Based on a 2-D Kunz cavitation model and standard k-e turbulent model for closure, a conventional finite volume method has been implemented with a SIMPLE algorithm on the collocated body-fitted grid in the present study. A validation check has been carried out by comparing with reference data of the impeller in a centrifugal pump. The results show a good agreement with reference values and can successfully provide the characteristics of cavitation on the blades of the impeller. A study of cavitation around the blades of target impeller supplying the fuel JP-7 is carried out. The role of the half-length blades in centrifugal pump impeller is also investigated. Calculation results confirm that the centrifugal pump design in this study was made free from cavitation if it operated within the design range. If the centrifugal pump operates due to temperature variation, the growth and depletion of cavitation are created among the blades and cause the instability of blade cascade. Moreover, the addition of three half-length blades plays an important role to get better operational characteristics of the impeller by reducing cavitation size, improving the cavitation free region and contributing the flow to be more stable through the elimination of high frequency flow oscillations.

Acknowledgment

This study was financially supported by Hanwha with KHP program. Authors greatly appreciate the financial grant for this work.

Nomenclature

α_l : Local void fraction
p, p_v : Static pressure, vapor pressure
μ : Kinetic viscosity
μ_t : Turbulent viscosity
u_i, u_j : Cartesian velocity components
x_i, x_j : Cartesian coordinates
δ_{ij} : Kronecker delta function
C_μ : Turbulent coefficient
S : Control surface
V : Control volume
t : Time
t_∞ : Time scale
k : Turbulent kinetic energy
ε : Dissipation rate
C_{dest} : Empirical constant
C_{prod} : Empirical constant
U_∞ : Free stream velocity
α_∞ : Angle of attack
S_t : Strouhal number
f : Frequency
C_L : Lift coefficient
c : Chord length of hydrofoil
d_1, d_2 : Blade inlet, outlet diameter
β_{s1}, β_{s2} : Blade inlet, outlet angle
h : Passage width
s : Blade thickness

z : Number of blades
n : Rotational speed
$\vec{n}$: Normal vector
$\vec{v}$: Velocity vector
$\vec{b}$: Body force vector
ρ_m, ρ_l, ρ_v : Density of mixture, liquid and vapor, respectively
$\dot{m}^+, \dot{m}^-$: Volume conversion rate of the condensation and of the evaporation

References

[1] D. Croba and J. L. Kueny, Numerical Calculation of 2D, Unsteady Flow in Centrifugal Pumps: Impeller and Volute Interaction, *International Journal for Numerical Methods in Fluids*, 22 (6) (1996) 467-481.

[2] J. S. Anagnostopoulos, Numerical Calculation of the Flow in a Centrifugal Pump Impeller Using Cartesian Grid, *Proceedings of the 2nd WSEAS Int. Conference on Applied and Theoretical Mechanics*, Venice, Italy (2006) 124-129.

[3] K. W. Cheah, T. S. Lee, S. H. Winoto and Z. M. Zhao, Numerical Flow Simulation in a Centrifugal Pump at Design and Off-Design Conditions, *International Journal of Rotating Machinery*, 2007 (2007) 1-8.

[4] F. Joussellin, Y. Courtot, O. Coutier-Delgosha and J. L. Reboud, Cavitating Inducer Instabilities: Experimental Analysis and 2D Numerical Simulation of Unsteady Flow in Blade Cascade, *4th International Symposium on Cavitation,* Pasadena, CA, USA (2001).

[5] Y. Iga, M. Nohmi, A. Goto, B. R. Shin and T. Ikohagi, Numerical Analysis of Unstable Phenomena of Cavitation in Cascade with Finite Blade Numbers, *Proc. 9th International Symp. on Transport Phenomena and Dynamics of Rotating Machinery*, Honolulu, Hawaii, USA (2002) 1-6.

[6] R. Fortes-Patella et al., A Numerical Model to Predict Unsteady Cavitating Flow Behaviour in Inducer Blade Cascades, *Journal of Fluid Engineering*, 129 (2) (2007) 128-135.

[7] O. Coutier-Delgosha, R. Fortes-Patella, J. L. Reboud, M. Hofmann and B. Stoffel, Experimental and Numerical Studies in a Centrifugal Pump With Two-Dimensional Curved Blades in Cavitating Condition, *Journal of Fluids Engineering*, 125 (6) (2003) 970–978.

[8] I. Senocak and W. Shyy, A pressure-based method for turbulent cavitating flow computations, *J. Comput. Phys.*, 176 (2) (2002) 363-383.

[9] C. Lee and D. Byun, Cavitation Flow Analysis of Axisymmetric Bodies Moving in the Water, *International Conference of Computational Science and Its Applications – ICCSA*, Glasgow, UK (2006) 537-545.

[10] O. Coutier-Delgosha, J. L. Reboud and G. Albano, Numerical Simulation of the Unsteady Cavitating Behaviour of an Inducer Blade Cascade, *Proc. ASME Fluids Engineering Summer Conference*, Boston Massachusetts, USA (2000).

[11] K. Okita, Y. Matsumoto and K. Kamijo, Numerical Analysis for Unsteady Cavitating Flow in a Pump Inducer, *5th International Symposium on Cavitation*, Osaka, Japan (2003).

[12] K. Majidi, Numerical Study of Unsteady Flow in a Centrifugal Pump, *Journal of Turbomachinery*, 127 (2) (2005) 363-371.

[13] Hiroki Ugajin, Masafumi Kawai, Kohei Okita, Takashi Ohta, Takeo Kajishima, Masataka Nakano and Hiroshi Tomaru, Numerical Analysis of the Unsteady Cavitating Flow in a 2D Cascade and a 3D Inducer, *43rd AIAA/ASME/SAE/ASEE Joint Propulsion Conference and Exhibit,* Cincinnati, Ohio, USA (2007) 5053-5063.

[14] F. C. Visser, J. J. H. Brouwers and J. B. Jonker, Fluid Flow in Rotating Low-Specific-Speed Centrifugal Pump Impeller Passages, *Fluid Dynamics Research*, 24 (1999) 275-292.

[15] O. Coutier-Delgosha, J. L. Reboud, N. Hakimi and C. Hirsch, Numerical simulation of cavitating flow in 2D and 3D inducer geometries, *International Journal for Numerical Methods in Fluids*, 48 (2) (2005) 135-167.

[16] R. F. Kunz et al., A preconditioned Navier-Stokes method for two-phase flows with application to cavitation prediction, *Computers & Fluids*, 29 (8) (2000) 849-875.

[17] I. Senocak, Computational methodology for the simulation of turbulent cavitating flows, *Ph.D. Dissertation*, University of Florida (2002).

[18] R. Fortes-Patella et al., Numerical Model to Predict Unsteady Cavitating Flow Behavior in Inducer Blade Cascades, *Journal of Fluids Engineering*, 129 (2) (2007) 128-135.

[19] D. Wilcox, *Turbulence modeling for CFD,* DCW Industries, Inc, La Canada, CA (1993).

[20] S. Patankar, *Numerical heat transfer and fluid flow,* Taylor & Francis, Kentucky, USA (1980).

Quangnha Thai received his B.S. in Aeronautical Engineering from Ho Chi Minh City University of Technology (HCMUT, Vietnam) and Ecole nationale superieure de mecanique et d'aerotechnique (ENSMA, France) in 2007. He is pursuing his M.S. in Aerospace Information Engineering from Konkuk University in Seoul, Korea. His research interests are in the area of computational fluid dynamics of two-phase flow and flow instability of rocket liquids.

Changjin Lee received his B.S. and M.S. in Aeronautical Engineering from Seoul National University in 1983 and 1985. He then went on to receive his Ph.D. from University of Illinois at Urbana-Champaign in 1992. Dr. Lee is currently a Professor at the department of Aerospace Engineering at Konkuk University in Seoul, Korea. His research interests are in the area of combustion instabilities of hybrid, liquid rocket and jet propulsions.